Dispensing of very low volumes of ultra high viscosity alginate gels: a new tool for encapsulation of adherent cells and rapid prototyping of scaffolds and implants

Michael M. Gepp[1], Friederike Ehrhart[1], Stephen G. Shirley[1], Steffen Howitz[2], and Heiko Zimmermann[1,3]

BioTechniques 46:31-43 (January 2009)
doi 10.2144/000113014

We present a tool for dispensing very low volumes (20 nL or more) of ultra high viscosity (UHV) medical-grade alginate hydrogels. It uses a modified piezo-driven micrometering valve, integrated into a versatile system that allows fast prototyping of encapsulation procedures and scaffold production. Valves show excellent dispensing properties for UHV alginate in concentrations of 0.4% and 0.7% and also for aqueous liquids. An optimized process flow provides excellent handling of biological samples under sterile conditions. This technique allows the encapsulation of adherent cells and structuring of substrates for biotechnology and regenerative medicine. A variety of cell lines showed at least 70% viability after encapsulation (including cell lines that are relevant in regenerative medicine like Hep G2), and time-lapse analysis revealed cells proliferating and showing limited motility under alginate spots. Cells show metabolic activity, gene product expression, and physiological function. Encapsulated cells have contact with the substrate and can exchange metabolites while being isolated from macromolecules in the environment. Contactless dispensing allows structuring of substrates with alginate, isolation and transfer of cell-alginate complexes, and the dispensing of biological active hydrogels like extracellular matrix-derived gels.

INTRODUCTION

The encapsulation of cells and drugs in small hydrogel spheres has been established over the past 10 years. Various techniques have been developed in this area ranging from airflow systems (1) to lab-on-chip microfluidic systems (2).

Encapsulation of insulin-producing islets of Langerhans (1) or metabolically active hepatocytes (3) in an alginate matrix provides implantable microbioreactors for regenerative medicine and drug delivery (4,5). Further applications for encapsulated cells can be found in the food industry (6), bioprocess engineering (7), pharmaceutical industries (8), and in cell culture (9). Alginate hydrogel capsules isolate embedded cells from the immune system or environment while allowing transport of O_2, nutrients, hormones, toxic metabolites, and CO_2 (Figure 1A). Hormones produced by encapsulated cells may pass through a matrix of suitable pore size. A technique capable of directly encapsulating adherent cells on substrates would be of great value, as cells suspended in hydrogel environments are round and not adherent. They cannot, for example, interact with extracellular matrix (ECM)–derived signal molecules, and therefore, intrinsic signal cascades are not triggered. However, these intrinsic pathways are crucial for cell survival, proliferation, migration, differentiation, and apoptosis (10). Proteins immobilized on surfaces like fibronectin, vitronectin, or laminin trigger signal transduction by binding to transmembrane receptors. Such signal cascades are very complex, but in the case of integrin receptors phospholipase Cs (PLCs), Ras proteins and phosphoinositide 3 kinases are phosphorylated and initiate gene transcription and the expression of gene products relevant to cell proliferation, differentiation, migration, or apoptosis (11). Cells that are removed from their natural environment often tend to apoptose (12), and fibroblasts in suspension are arrested in the G phase of the cell cycle and cannot proliferate (13–15).

In this paper, we present a new method and device for encapsulating cells in clinical-grade alginate while allowing them to adhere to surfaces and receive chemical signals (see Figure 1B). The system dispenses high-viscosity liquids and allows selection of the points of interest to be encapsulated. We show first proof-of-concepts for several applications in biotechnology.

MATERIALS AND METHODS

Alginate Dispenser System

We designed a completely new system for dispensing ultra high viscosity (UHV) alginates. At the core, a modified micrometering valve (commercially available by DELO Industrial Adhesives GmbH, Windach, Germany, and modified by GeSiM, Rossendorf, Germany) is integrated into an xy-table Nano-Plotter (GeSiM). The heatable micrometering valve is controlled by DELO-MAT (DELO Industrial

[1]Fraunhofer Institute for Biomedical Engineering, St. Ingbert, Germany, [2]Gesellschaft für Silizium-Mikrosysteme mbH GeSiM, Rossendorfer Technologiezentrum, Großerkmannsdorf, Germany, and [3]Saarland University, Saarbruecken, Germany

Adhesives GmbH), which controls the piezo-actuator (stack) of the valve. The alginate reservoir is a luer-lock syringe connected to a precision pressure controller and pressure source. An additional technical industrial miniature video microscope T.I.M.M. 150 (SPI GmbH, Oppenheim, Germany) fixed on the xy-table allows in-process inspection and selection of targets. Figure 1C illustrates the general setup of the system. A dilutor as part of the Nano-Plotter transports fluids to a wash station on the xy-table. The DELO-Dot alginate dispenser and Nano-Plotter are linked to a personal computer with appropriate Nano-Plotter software NPC16 (GeSiM) that allows the control of the system and the editing of individual dispensing procedures. A light source (Fiber Illuminator; Nikon, Düsseldorf, Germany) and pump complete the system and facilitate handling of biological samples during encapsulation procedures. A laminar flow hood keeps the system sterile.

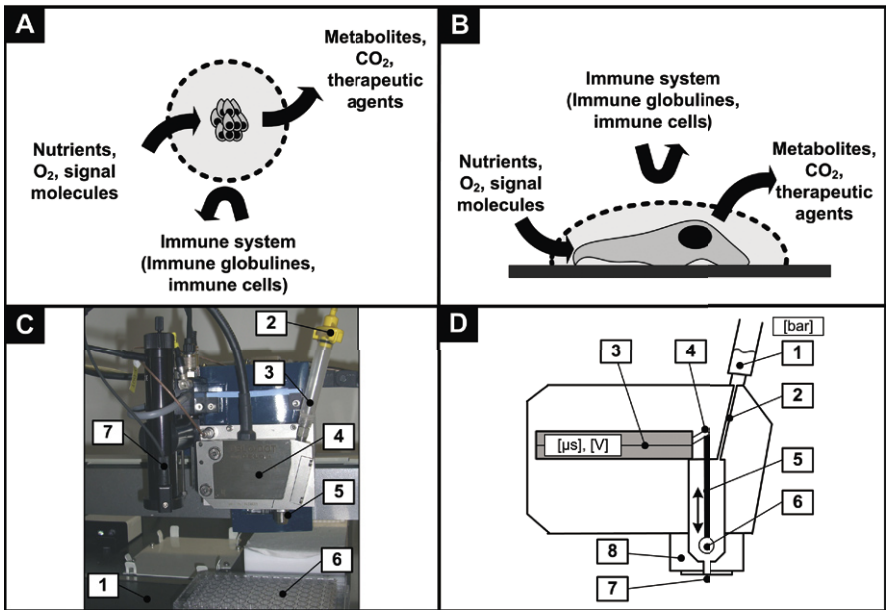

Figure 1. Two-dimensional (2-D) encapsulation and technical details. (A) Encapsulated cells in a gel matrix such as alginate can exchange oxygen, nutrients, toxic metabolites, and therapeutic agents with the environment while being protected against the immune response of a host. (B) 2-D encapsulation allows the immobilization and isolation of adherent cells. In addition, physical and chemical signals on the surface can trigger membrane receptors and, ultimately, gene expression (i.e., of anti-apoptotic genes). (C) The alginate-dispensing system consists of the xy-table Nano-Plotter [1], air pressure interface [2] linked with alginate reservoir syringe [3], the piezo-driven micrometering valve [4], the faceplate with 200-µm outlet [5], the well plate (e.g., with adherent cells) [6], and the technical industrial miniature microscope [7]. Not shown are the pump system for the removal of media, the light source, the dilutor, the valve control unit, and the precision pressure controller. (D) Details of the micrometering valve: the alginate reservoir [1] is connected with the alginate inlet channel [2] to the inner valve. The piezo-actor [3] is linked over a toggle [4] to a needle [5]. The small ceramic sphere [6] on the end of the needle seals the output [7] of the removable faceplate [8]. Voltage and pulsewidth for the piezo-actor and pressure are controllable parameters.

Table 1. Dried Alginate Spot Size of Different Dispenser-to-Substrate Distances and Substrates

Faceplate-to Substrate Distance (mm)	Area (mm^2)		
	Polystyrene	Glass	Polysine
5	0.03 ± 0.01	0.90 ± 0.25	2.26 ± 0.24
7	0.03 ± 0.02	0.32 ± 0.32	1.55 ± 0.40
15	0.01 ± 0.01	0.14 ± 0.16	0.89 ± 0.23

Table 2. Metabolic Activity Estimated by WST-1 Assay

Time (h)	$Absorbance_{450nm}$ (-)		
	Encapsulated Cells	Positive Control	Negative Control
0.5	1.6 ± 0.3	2.0 ± 0.1	0.8 ± 0.0
2.0	8.2 ± 1.0	8.7 ± 0.3	6.6 ± 0.2
4.5	13.2 ± 1.0	14.4 ± 0.4	10.9 ± 0.2
6.5	14.5 ± 1.0	14.7 ± 0.0	11.4 ± 0.4
22.5	13.0 ± 1.9	13.2 ± 1.1	12.1 ± 1.0

Micrometering Valve

The micrometering valve consists mainly of 034, 301, and 305 stainless steel. The integrated sealing system is a zirconium oxide ceramic component (Chemraz, Greene, Tweed, Hofheim am Taunus, Germany). Microvolumes are dispensed by a piezo-actuated mechanism. Alginate flows in the inner chamber of the valve under pressure from the syringe. Normally, a small ceramic sphere connected by a needle to the piezo-actuator seals the output channel. To dispense one or more spots, the PC sends signals with user-defined parameters (pulsewidth, voltage, and frequency) to the valve and position instructions to the xy-table. The piezo-actuator contracts, the needle moves up, and the ceramic sphere opens the output. The piezo-actuator relaxes after a given pulsewidth and moves the ceramic sphere downward. The movement ejects fluid with high velocity. The dispensing of more than one spot can be controlled by the frequency parameter, and the manufacturers claim that fluids with viscosities in the range of 50–200,000 mPas can be dispensed. Figure 1D is a drawing of the valve, which produces small cylindrical jets.

UHV Alginate

The alginate was extracted from *Lessonia nigrescens*, which has a high proportion of β-D-mannuronate (M) (60%), and from *Lessonia trabeculata*, high in α-L-guluronate (G) (90%). Algal stipes, harvested from the Chilean coast, were peeled and cleaned. After antimicrobial treatment and chopping, alginate

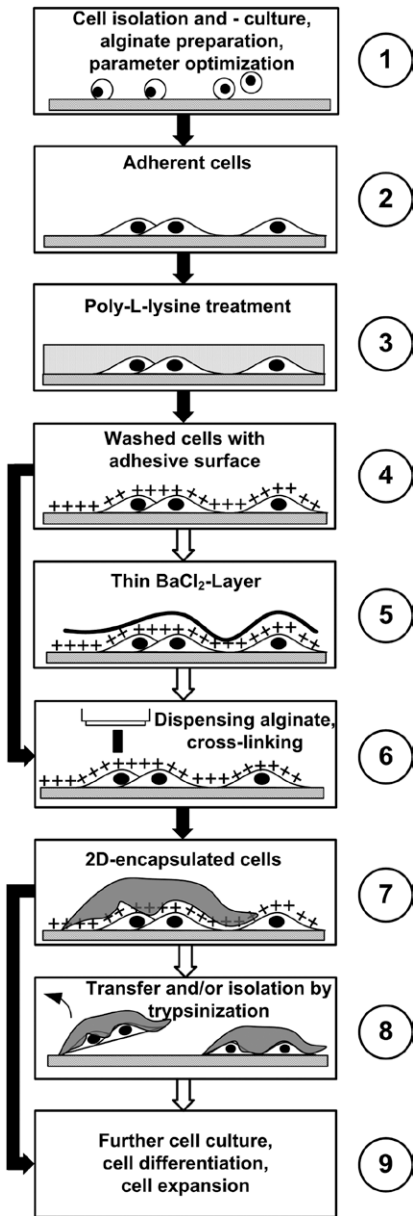

Figure 2. General encapsulation pipeline for adherent cells. Sequential main flow of encapsulation, indicated by black arrows, can be varied at two points, indicated by white arrows.

was extracted with Ca^{2+}-chelating agents and debris was removed by filtration. The product was purified by repeated ethanol precipitation and resolution and finally air-dried or lyophilized and stored at 4–8°C. Further details are given in Reference 1. Experiments utilized mixtures of the two alginates, which were dissolved separately in NaCl (0.9% w/v) for at least 12 h and mixed 1:1 (v/v) just before use. The choice and concentration of cross-linking agent, cross-linking time, and polymer concentration can tune the mechanical properties of the resulting hydrogel.

Cell Culture

For our main studies, we used L929 fibroblasts, murine neuroblastoma cells, human prostate carcinoma cells, Caco-2 cells, and human hepatocellular carcinoma cells as cell models. L929 fibroblasts and Caco-2 cells (both from DMSZ, Braunschweig, Germany) were cultivated with Dulbecco's modified Eagle media (DMEM; Fisher Scientific, Karlsruhe, Germany) containing 10% sterile filtrated fetal bovine serum (FBS) (LGC Promochem, Wesel, Germany) and 1% gentamycin (Sigma Aldrich Chemie, GmbH, Schnelldorf, Germany). Murine neuroblastoma 2a cells (DMSZ) were cultivated with DMEM containing 10% FBS. Human prostate carcinoma cells (PC-3; DMSZ) were cultivated with RPMI 1640 (LGC Promochem) and Ham's F12 (in a ratio of 1:1; PAN-Biotech GmbH, Aidenbach, Germany) containing 10% sterile filtrated FBS and 1% gentamycin. Human hepatocellular carcinoma cells (Hep G2; LGC Promochem) were cultivated in RPMI 1640 containing 10% sterile filtrated FBS. All cells were cultivated at 37°C, 95% relative humidity, and 5% CO_2.

(Bio-) Chemicals

The cross-linking solution was 20 mM $BaCl_2$, 115 mM NaCl (both from Sigma Aldrich Chemie GmbH), and 5 mM L-histidine (Merck, Darmstadt, Germany). The solution was sterilized by filtration.

Saline was NaCl (0.9%, w/v; Sigma Aldrich Chemie GmbH) in ultra-pure water and sterilized by filtration.

Poly-L-lysine solution (0.01%; Sigma Aldrich Chemie GmbH) was diluted with 1× phosphate-buffered saline (PBS; Sigma Aldrich Chemie GmbH) to obtain concentrations of 0.001%, 0.00075%, 0.0005%, and 0.0001% (v/v).

Live/dead staining solution for cell models contained 5 mL basal media without supplements with 8 µL fluorescein diacetate (FDA; 5 mg/mL in acetone) and 50 µL ethidium bromide (EB; 1 mg/mL in pure water).

Alcian blue 8GX (Sigma Aldrich Chemie GmbH) was dissolved thoroughly in ultra-pure water before sterile filtration. ECM gel from Engelbreth-Holm-Swarm murine sarcoma (Sigma Aldrich Chemie GmbH) was diluted by serum-free DMEM 1:10 and handled at approximately 4°C to avoid rapid gelling.

WST-1 cell proliferation reagent (Roche, Mannheim, Germany) was used (10% in culture medium) to determine metabolic activity of immobilized cells.

For immunostaining of cells, Alexa Fluor 488 goat anti-mouse immunoglobulin G (IgG, 1% in PBS; Molecular Probes, Invitrogen, Karlsruhe, Germany), goat serum (2% in PBS), monoclonal anti-cytokeratin peptide 8 antibody (produced in mouse, 1% in PBS), and methanol cooled to -20°C (all purchased from Sigma Aldrich Chemie GmbH) and HEPES buffer (Gibco, Fisher Scientific) were used.

Characterization of Dispensed Volumes

For alginate and NaCl-solution, 500 jets were dispensed into a tube and weighed for each particular set of parameters and alginate concentration. In addition, the dispensing process was observed by a high-speed video analysis system SpeedCam Visario LT400 (Weinberger Vision, Erlangen, Germany).

Determination of Spot Size

The influence of hydrophilicity of substrate was analyzed by comparing spot areas. We used polystyrene, untreated glass, and glass treated with Polysine (Sigma Aldrich Chemie GmbH) as substrates. These surfaces rank in hydrophobicity such that polystyrene > glass > Polysine-treated glass. We produced a spot pattern of sodium-alginate (0.7%, w/v, 1:1 mixture *L. trabeculata* and *L. nigrescens*) solution. Areas of the dried spots were determined by the software package ImageJ (rsbweb.nih.gov/ij, National Institutes of Health, Bethesda, MD, USA; Reference 16).

Optimizing Poly-L-lysine Treatment

We optimized surface treatment using different concentrations of poly-L-lysine in combination with different cell models. Adherent cells were incubated for 15 min in poly-L-lysine solutions 0.001%, 0.00075%, 0.0005%, 0.0001%, and 0% (v/v) at 37°C and 5% CO_2. After

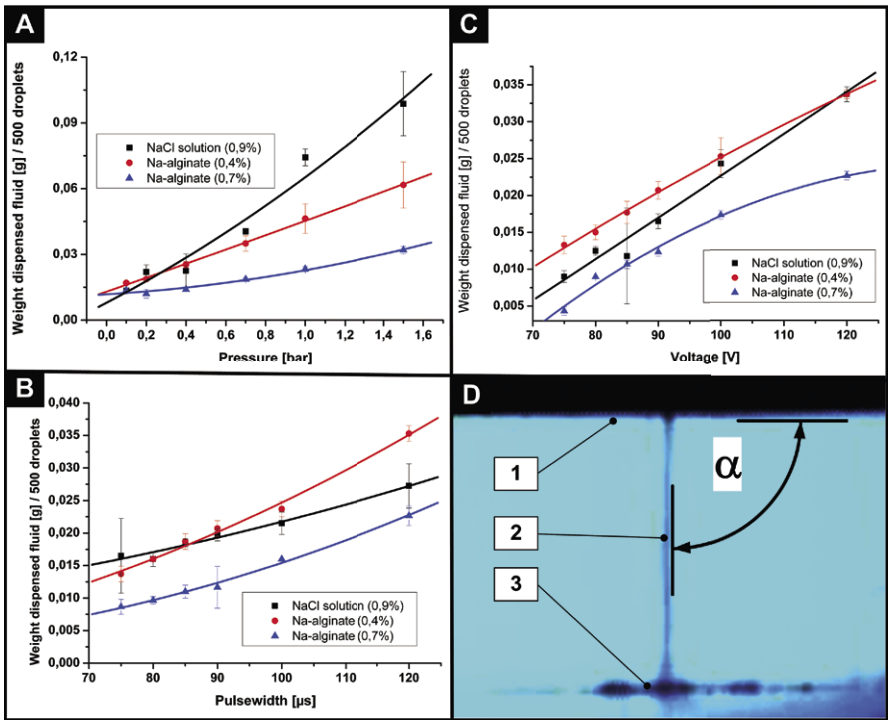

Figure 3. Characterization of the system. (A) Weight of 500 spots [g] 0.7% alginate, 0.4% alginate, and NaCl solution versus pressure [bar], (other applied parameters are 90 V and 90 µs). (B) Weight of 500 spots [g] 0.7% alginate, 0.4% alginate, and NaCl solution versus pulsewidth [µs] (other applied parameters are 0.2 bar and 90 V). (C) Weight of 500 spots [g] 0.7% alginate, 0.4% alginate, and NaCl solution versus voltage [V] (other applied parameters are 90 µs and 0.2 bar). Error bars indicate variability of weight ($n = 3$). (D) High-speed pictures of dispensing procedure. The alginate dispenser generates a jet rather than a droplet. The jet normally leaves the valve at an angle $\alpha = 90°$. (Faceplate and output [1], alginate jet [2], and site of impact [3]).

that, cells were washed with PBS, and vitality was determined by live/dead staining and fluorescence microscopy.

Development of Two-dimensional Encapsulation Process of Adherent Cells

After characterizing the system, we developed an encapsulation procedure for adherent living cells. Adherent cells, a surface adhesive for alginate and a cross-linking procedure are necessary for the encapsulation process. Cells were seeded in standard cell culture dishes with a concentration of 25,000–40,000 cells/cm^2. Cells were cultivated for ≥2 h to achieve adherence. After culture, the medium was removed, and the cells were rinsed with PBS. In another step, cells were coated with poly-L-lysine solution (0.0005%, v/v) to functionalize cells and substrate surface with positive charges for interaction with alginate. After incubation, poly-L-lysine was removed, and the sample was rinsed with PBS. During encapsulation, the cross-linking ($BaCl_2$) solution layer over the cells has to be as thin as possible, while ensuring that cells do not become dry. Alginate was dispensed with appropriate pressure (0.2 bar), pulsewidth (90 µs), voltage (90 V), and distance from faceplate to substrate (30 mm). Alginate was cross-linked by carefully flowing $BaCl_2$-solution over the substrate. Alcian blue 8GX was added for staining cross-linked alginate, and after an incubation time of 15 min, the cross-linking agent and alcian blue were removed, and cells were rinsed twice with PBS (see Figure 2A, steps 1–4, 6, and 7). The selected incubation time was based on the known Ba^{2+} inhibition of transmembrane potassium channels. Cells were stained for vitality and examined with fluorescence microscopy.

Development of Further Applications: Dispensing Biological Relevant Fluids and Structuring of Substrates

ECM gel diluted 1:10 (v/v) was loaded into a syringe and screwed onto the inlet interface of the alginate dispenser. Parameters were optimized for this liquid gel, and a spot matrix was dispensed on untreated cell culture dishes (Corning, Lowell, MA, USA). After 30 min drying of gel, L929 cells were seeded onto substrates and cultivated at standard conditions (37°C, 5% CO_2) for 24 h. Samples were further analyzed by brightfield microscopy (Eclipse TE 300 fluorescence microscope; Nikon).

Structuring of Polysine-pretreated glass slides was performed by dispensing a spot matrix of 0.7% NT-alginate onto the surface. Alginate adheres to these slides, and no pretreatment is necessary. Alginate was cross-linked for 15 min with 20 mM $BaCl_2$ solution, and slides were rinsed with 1× PBS. L929 fibroblasts were seeded and cultivated for 24 h at 37°C and 5% CO_2.

Cleaning of the Micrometering Valve

After every encapsulation procedure, we cleaned the valve with ultra-pure water and dried it with compressed air. Periodically, we cleaned the valve with standard cleaning-in-place (CIP) chemicals to avoid or remove corrosion triggered by chloride ions. The faceplate and inner chamber of the valve were cleaned with Steris CIP 200 (phosphoric and citric acid) for 15 min, rinsed with ultra-pure water, repassivated with RP Pharma RTU (nitric acid and citric acid) for 15 min, and rinsed again with ultra-pure water. Both chemicals were from Ateco Services AG, Rheinfelden, Switzerland.

To maintain sterility, both the inner valve and the faceplate can be treated with 70% ethanol before the encapsulation. Sterilizable luer-lock syringes supply the system with medical-grade sterile UHV alginate, and the plotter is installed in a laminar flow hood.

Behavior Studies of Adherent Encapsulated Cells

L929 fibroblasts encapsulated under spots were analyzed by a live cell imaging system Biostation IM (Nikon). The substrate was placed in the sample incubation chamber and cultivated at 37°C and 5% CO_2. Encapsulated and nonencapsulated cells were investigated under software control for 24 h. Resulting movies of selected sites were analyzed using imaging processing software IrfanView (www.irfanview.net)

and ImageJ. For this purpose, pictures were exported every hour for 15 h, and cell shape outlines and overlay pictures were generated. Further investigation of cell behavior and long-term cultivation (1 week) of encapsulated L929 fibroblasts was performed by manual movie inspection.

The proliferation time of adherent fibroblasts under alginate spots was estimated by manual analysis of time-lapse movies taken by Biostation IM for 20 h. In addition, motility of fibroblasts (encapsulated and nonencapsulated) was estimated by measuring the covered distance over time by tracking the position of cell nuclei. Therefore, time-lapse movies were analyzed by the ImageJ plugin "Manual tracking," and average distances of cells were calculated. The encapsulation of fibroblasts with UHV alginate (0.7% NT) was performed by our optimized parameters.

Estimation of Functionality and Metabolic Activity of Immobilized Cells

General metabolic activity after immobilization was determined using a WST-1-based colorimetric assay. The WST-1 assay was also performed using the PC-3 human cell line. Cells (2×10^5) in a 35-mm dish were cultivated for several hours, and the standard immobilization protocol ("sample") was used for dispensing alginate onto cells. As a positive control, cells were treated with poly-L-lysine and $BaCl_2$, and for the negative control, PBS was dispensed with high pressure so that cells were ablated at the impact point (just before the WST-1 assay). Samples were incubated in culture medium with WST-1 reagent in an incubator. Small volumes (triplets) of gently mixed supernatant were taken after 0.5, 2.0, 4.5, 6.0, and 22.5 h, and absorbance was measured at 450 nm.

Cytokeratin Expression After Immobilization

Cytokeratin expression was measured 24 and 48 h after immobilization. Immobilized human prostate carcinoma cells (PC-3) were treated with methanol and incubated with goat serum containing murine anti-cytokeratin primary antibodies. Cells were treated with Alexa Fluor goat anti-mouse secondary antibodies, incubated in Hepes buffer, and observed by fluorescence microscopy.

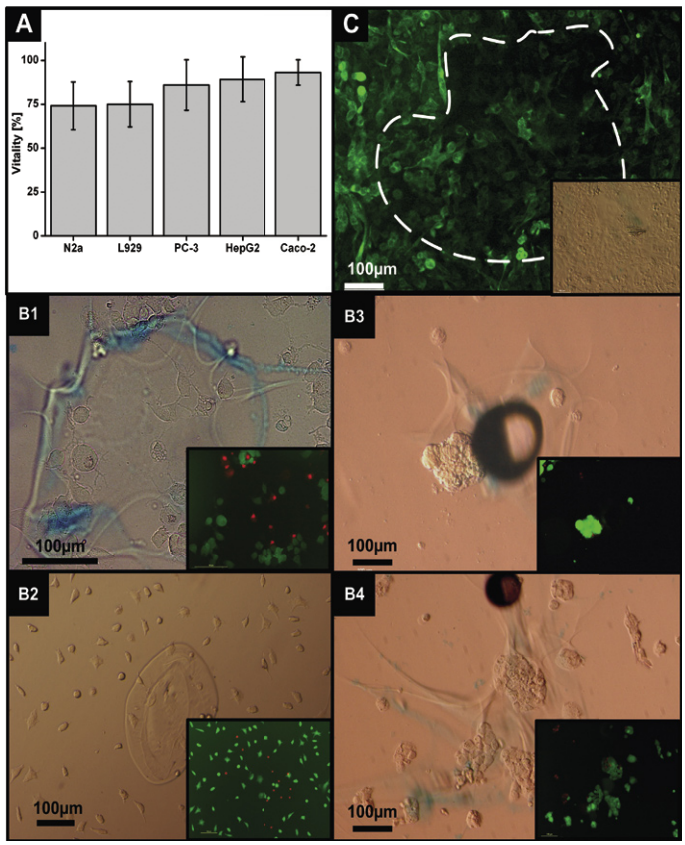

Figure 4. Encapsulation of adherent cells. (A) Viability of different cell lines under alginate spots after encapsulation. All cell lines used in the study show viabilities >70%. Best viabilities are for cell lines Hep G2 or Caco-2 growing in a colony-like manner ($n = 3$ experiments). (B) [1] Encapsulated N2a cells immediately after encapsulation. Superfine processes of N2a were not damaged by encapsulation. Alginate is stained by alcian blue. Inset: cell viability test. [2] Encapsulated L929 fibroblasts after encapsulation of cells coated by a thin $BaCl_2$ layer. Inset: live/dead staining. [3] Encapsulated Caco-2 cells. Cell cluster under alginate (stained by alcian blue) show excellent viability. Inset: live/dead staining. [4] Encapsulated Hep G2 cells. Cell aggregates under alginate spots (stained by alcian blue) show excellent vitalities. Inset: live/dead staining. (C) Immunostaining of alginate spot region [used filter: fluorescein isothiocyanate (FITC)]. Cytokeratin is detected 48 h after the encapsulation procedure at PC-3 cells under alginate and documents the general functionality of gene apparatus (gene transcription and translation). Inset: brightfield microscopy picture of encapsulated region.

RESULTS

Dispensing UHV Alginate and Process Preparation

The dispenser system can handle sodium alginates of concentrations between 0.4% and 0.7% (w/v) and also low viscosity fluids like NaCl solution or ECM-derived gels. The system allows the usage of a variety of substrates, ranging from glass slides to 96-well plates. Biological samples can be handled without problems in the laminar flow hood. After cleaning, there are no visible rouging sites on stainless steel surfaces, needle, and interior faceplate. Rouging and rust deposits on ceramic parts (sealing system) were also removed without influencing leak-tightness of the valve. Rouging-linked desorption of small rust particles or red coloration of alginate during dispensing were not observed after introduction of the cleaning procedure. Figure 3A shows the amounts of alginate versus applied pressure. From 0.1–0.2 bar, dispensed volume of different fluids is quite similar and is about 0.02 g/500 droplets. At higher pressures, dispensed volume is proportional to pressure. Dispensed volume decreases with increasing viscosity. The shapes of the volume-pulsewidth curves (Figure 3B) for 0.7% alginate and 0.4% alginate are similar,

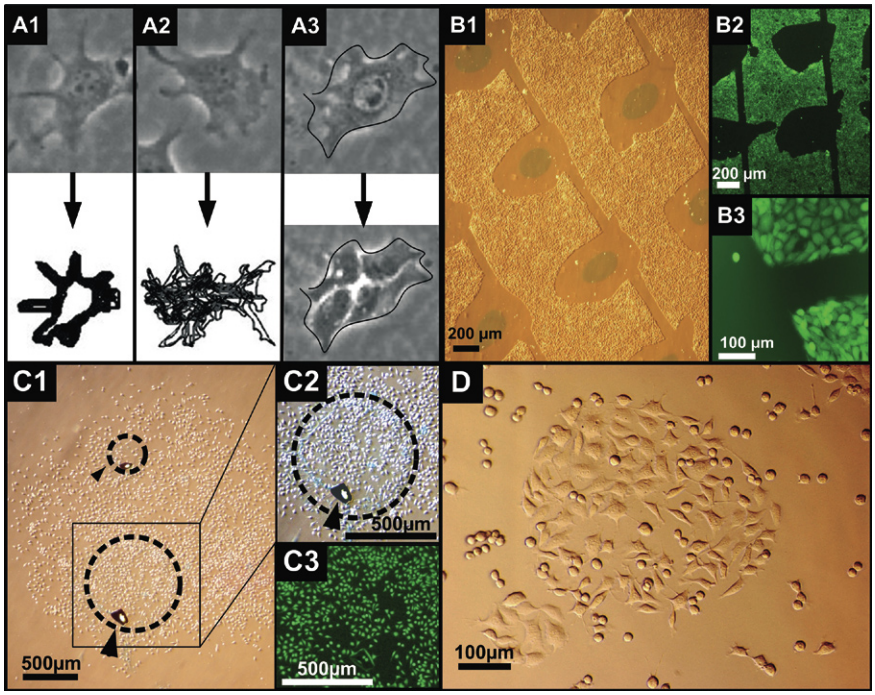

Figure 5. Applications realized with alginate dispenser. (A) [1] Time-lapse movies over 15 h of L929 cells under alginate layer. There is little change in cell shape and no migration. [2] Nonencapsulated fibroblasts. The cell changes shape. [3] Encapsulated L929 fibroblasts after two cell cyles (19 h). All cells have to share the volume of the initial encapsulated cell and are close to each other. Black line projects initial cell shape on divided cell colony. (B) [1] Alginate patterned substrates realized by alginate dispenser. The brightfield microscopy picture shows alginate spot matrix on a Polysine slide after a 24-h cell culture with L929 fibroblasts (detail). Microscopy images show that fibroblasts are not growing in areas coated with alginate. Channels between single spots occur due to moving of faceplate from one point to another. [2] Fluorescence picture [fluorescein diacetate (FDA)–stained, fluorescein isothiocyanate (FITC) filter] shows another site of structured substrate (2× magnifications). [3] Higher magnification (20×) of alginate stripe with sharp edges. (C) [1] Mask-assisted cell immobilization. Small cell spots are produced by pipetting a defined pattern. Replication of the same pattern by alginate dispenser gives small cell spots including encapsulated regions. [2] Closer view of encapsulated region of [1]. Bar indicates scale of 500 µm; arrow tips indicate air bubbles. [3] Encapsulated region after staining by FDA (fluorescence picture, FITC filter). (D) Biological relevant fluids like extracellular matrix (ECM)–derived gels can also be handled with the dispenser. After cell culture regions with ECM, spots can be observed due to characteristic adherent cells and higher cell densities in spot regions (microscopy image, 20× magnifications).

although different from that for NaCl. Figure 3C shows dispensed mass of solutions versus voltage, V. The slope between 75 and 90 V is nearly identical for all three fluids. Above about 90 V, the slope of 0.7% alginate decreases. NaCl solution can be dispensed, although the mass is less than that for 0.4% alginate. From these results, we can estimate the volume of a single spot (jet). The mean volume of one jet of 0.7% alginate is about 20 nL, with parameters of 90 V, 90 µs, and 0.2 bar. With the same parameters, the volume per spot for 0.4% alginate is 40 nL.

Higher volumes can most easily be achieved by increasing pressure. At 1.5 bar, volume per spot is 120 nL for 0.4% alginate and 60 nL for 0.7% alginate.

Figure 3D illustrates the ejection of a single alginate jet. Normally, the jet leaves at an angle, $\alpha = 90°$, and impacts the surface at the same angle. However, we could sometimes observe output angles that differed from 90° in high-speed movies. The cause was small particles partly blocking the valve's outlet and deflecting the jet.

Table 1 shows the mean spot size variation with height (outlet-substrate distance) and substrate hydrophilicity. The spots get smaller with increasing height, regardless of the physical properties of the surface. The smallest spots were on the hydrophobic polystyrene surface, and the largest spots were on the hydrophilic Polysine. While there is high variance, this a simple method for forming spots with small volumes.

Encapsulation of Adherent Cells

The process and current hardware gives a cell viability for L929 fibroblasts of 68% (±19%) with parameters 90 V, 25 Hz, 90 µs, 0.2 bar, dispenser-to-substrate distance of 30 mm, and 0.7% UHV. The application of a thin medium layer (100 µL on 1.9 cm^2 well surface) over cells before encapsulation can improve viability up to 89%. Encapsulation of L929 fibroblasts with current hardware gives cell viabilities of 25–90% per spot. The overall viability is about 75% (±13%). High variance of viability results from heterogeneous spot sizes (see Table 1) and splash erosions produced by current parameters and hardware. Similar results were obtained with encapsulation of neuroblastoma 2a cells (74% ± 14% vital cells, see Figure 4B1), and PC-3 cells (86% ± 14% vital cells) under spots could be observed. Best encapsulation results (Figure 4A) are observed with Hep G2 (89% ± 13%) and Caco-2 cells (93% ± 7%).

In our study, L929 fibroblasts, murine embryonic fibroblasts (MEF), and murine neuroblastoma cells (N2a) were subjected to different poly-L-lysine concentrations at 37°C for 20 min to optimize poly-L-lysine concentration. The vitality of MEF fell from 100% at 0% poly-L-lysine to 49.88% (± 2.80%) at 0.001% poly-L-lysine. Vitality of N2a fell from 99.01% (±1.38) at 0% poly-L-lysine to 56.85% (± 8.95%) at 0.001% poly-L-lysine. Vitality of L929 fibroblasts fell from 100% at 0% poly-L-lysine to 81.75% (± 4.6%) at 0.001% poly-L-lysine. L929 fibroblasts are not as susceptible as MEF or N2a cells. The concentration of poly-L-lysine actually used (0.0005%) gave a viability for L929 of 96%.

When adherent cells were encapsulated and then treated with trypsin, the result depended on the cell density. At high densities, the cell alginate complex detached from the substrate and could be transferred to another vessel. At low densities, the complex remained attached to the substrate, and small cell-alginate patterns were produced. However, an ultra-thin film of $BaCl_2$ solution can cross-link alginate directly upon impact (compare Figure 4B2) without affecting hydrogel adhesion to

substrate. A further advantage of this approach is the avoidance of air bubbles (which are present in spots in Figures 4B3 and 4B4). Air bubbles impede mass transfer and can be lethal to cells.

Patterning with Cells and Fluids

Figures 5C1–5C3 show the results of miniaturizing the encapsulation process. Because of the excellent precision and reproducibility of the xy-table, small groups of adherent cells can be encapsulated with patterns of alginate. On Polysine slides, an ultra-thin alginate layer seems to form a nonadherence site for cells. Seeding of cells was performed after cross-linking and rinsing of structured substrates. After 24 h, cells are adherent at uncoated sites but not at alginate-coated sites. Alginate inhibits adhesion (17).

Figures 5B1 and 5B2 show structured Polysine slides with adherent L929 fibroblasts after 24 h of cultivation. Cultivation of cells also reveals covered regions that are not alcian blue–stained. There are also unstained areas without adherent cells. It seems that these regions are also covered with an ultra-thin alginate layer and therefore not detectable by alcian blue staining. Nevertheless, a more detailed view of the cell-alginate interface in Figure 5B3 reveals excellent discrimination between coated and uncoated regions. Besides alginate, the dispensing system is also able to dispense other viscous fluids, such as ECM-derived gels as patterns. Figure 5D shows adherent cells anchored to ECM gel on the surface. ECM provides optimal growth conditions for fibroblasts.

Proliferation of Encapsulated Cells Under Time-lapse Microscopy

Time-lapse analysis revealed that encapsulated L929 cells remain adherent and, despite alginate impact, do not detach from the surface. The gel limits the space available for cells. Daughter cells have to assume the shape of the parent (Figure 5A3), and cell shape remains nearly constant over time. Figure 5A1 shows the shape analysis of one encapsulated cell (overlay picture of cell shapes) and illustrates that filopodia tend to remain in the same place. This behavior could be observed for all encapsulated L929 fibroblasts. In contrast, cell shape and cell surface of nonencapsulated fibroblasts is extremely variable (Figure 5A2).

Nonencapsulated fibroblasts cover an average distance of 134.1 µm (±22.9 µm) during 20 h, whereas encapsulated fibroblasts cover an average distance of just 33.8 µm (±2.4 µm). Cell division takes place after 12.6 h (±2.6 h) under alginate spots and after 10.7 h (±5.05 h) with nonencapsulated fibroblasts. Overall, cell division took place at least once in 91.5% (±9.2%) of encapsulated and in 94.4% (±22.9%) of nonencapsulated cells during the 20 h (see also Figure 5A3).

Long-term cultivation of encapsulated L929 fibroblasts monitored by time-lapse microscopy verified the sterility of the procedure. No observable bacterial contamination occured during the 1 week following encapsulation.

Functionality and Metabolic Activity of Immobilized Cells

Table 2 shows the metabolic activity of PC-3 cells after encapsulation in comparison to nonencapsulated cells (positive control) and ablated cells (negative control). Overall, there are only small differences in the activity of encapsulated cells and the positive control, whereas the negative control shows the lowest metabolic activity of cells.

Immunhistochemistry of encapsulated PC-3 cells shows the expression of cytokeratin (see Figure 4C) after dispensing alginate, and thus the functionality of the gene expression apparatus.

DISCUSSION

Stainless steel does suffer from corrosion triggered by Cl^- ions. However, with proper cleaning and passivation, sterile dispensing is quite possible. Despite very careful dispensing, flow of cross-linking agent deforms alginate spots (not shown), producing thin processes.

We have successfully encapsulated adherent murine L929 fibroblasts; neuroblastoma cells N2a; PC-3, Caco-2, and Hep G2 cells; and, in early experiments, MEFs and primary chicken cardiomyocytes with the same encapsulation process. Excellent vitality of Caco-2 and Hep G2 cells can be explained by cell morphology, particularly the scattered colony-like growth.

In the described process, poly-L-lysine treatment is critical. Poly-L-lysine is associated with apoptosis (3,18), but as a cationic agent, promotes adhesion. At incubation times of 20 min and concentrations of 0.0005%, poly-L-lysine allows high vitality and provides excellent alginate adhesion. Nevertheless, future work will consider alternative cationic agents like poly-L-ornithine, poly-D-lysine, and low–molecular weight poly-L-lysine.

The ablation forces of raindrop impact are well known. If a droplet cannot penetrate, water flows sideways with up to double freefall velocity and generates high shear stresses and erosion (see also Reference 19). Incoming jets may have a velocity of ~8 m/s (revealed by high-speed movies) and generate lateral velocity of ~16 m/s. The kinetic energy is mainly affected by voltage. Velocity increases from ~3 m/s at 85 V to ~9 m/s at 95 V, and there is also an increase in mass. Increasing voltage from 70 to 90 V increases the kinetic energy of drops by ~6–7 J.

Cells can be damaged by the high shear stresses and moved to edges of the alginate spot. Geologically, a water layer minimizes splash erosion of soil (20), and the same principle seems to hold with a thin layer of $BaCl_2$ or medium protecting cells. Optimal survival was found by dispensing alginate with low settings for all parameters. Decreasing volume means that the jet pressure on the impact area gets minimized, and the cells are not abused in the area where the jet hits the substrate. Following this strategy minimizes splash erosions (ablation of cells). Parameters influencing volume are voltage, pulsewidth, pressure, and viscosity. The distance between the faceplate and the valve does not influence the volume, but it also seems to affect encapsulation results, probably by scattering of the jet. At faceplate-to-substrate distances of >25 mm, we could observe small spots, called satellites, that probably originate from jet fragmentation (Table 1).

Figure 3, A–C shows that the dispensed volume of alginate depends on concentration and viscosity. Increasing viscosity decreases dispensed volume.

Volumes are also reduced by reducing pressure, pulsewidth, or voltage. Pulsewidth controls the duration of valve opening and voltage controls its extent. They both influence the acceleration of the fluid. Pressure affects the viscous flow. NaCl solution behaves differently from alginate; however, it has a viscosity outside the valve manufacturer's recommended range. While the dispensing of low viscosity fluids has to be carefully checked, pressure can be used to control output.

Time-lapse movies show that encapsulated cells are vital and can proliferate. After two divisions, four cells have to share the place of the initial cell (Figure 5A3). The behavior of rapidly dividing cells in such an environment needs further investigation. The production of small cell agglomerates and cell fusion chambers is possible. Because some cell types (like murine embryonic fibroblasts) can leave the spot, encapsulation research should consider novel substrates (e.g., with micro- and nanostructures) that inhibit cell movement.

Encapsulated cells had reduced mobility but similar proliferation time and competency when compared with nonencapsulated ones. The motility of free, nonencapsulated fibroblasts is limited by hurdles such as contiguous cells or particles on the substrate. The highest motility of free fibroblasts could be observed directly after cell division. In contrast, motility of encapsulated fibroblasts is strongly restricted by the surrounding alginate gel. In this case, the covered distance in 20 h averages <40 µm. After proliferation, encapsulated daughter cells must share the initial space in the alginate. The investigation of proliferation reveals that cell division takes place even after the encapsulation procedure. Regarding the general proliferation competency, it seems that there are no significant differences between encapsulated and nonencapsulated cells; we could observe cell cycles in >90% of cells in both cases. The shift of the starting point of proliferation of about 2 h probably originates from stress during the encapsulation procedure. The short doubling time of <15 h in both populations should be further investigated due to the cited doubling time of 21–24 h by DMSZ.

In addition to proliferation of L929 fibroblasts, encapsulated PC-3 cells show a comparable functionality concerning gene product expression (cytokeratin peptide 8) and general metabolic activity to nonencapsulated cells. The verification of cytokeratin peptide 8 by immunhistochemical staining after the encapsulation procedure of cells under alginate leads to the conclusion that the gene expression apparatus (gene transcription and translation) of encapsulated cells is still functional. We conclude that this observation is transferable to other cell lines and gene products (i.e., pancreatic cells and insulin). The encapsulation of primary chicken cardiomyocytes by our system (data not shown) and the contraction of cell clusters 1 week after encapsulation is a good indication of the functionality of immobilized cells and a putative wide spectrum of future applications in biotechnology and regenerative medicine.

The alginate dispensing system allows rapid prototyping. Components used in the system are characterized by the highest flexibility concerning culture vessels, encapsulation medium, and desired spot layout. Modular parts of the dispenser unit can be easily modified and adapted. In this manner, a small plate with a 50-µm hole (a small etched silicon disc) is glued in front of the faceplate (Figure 1D, part 7). The variation of outlet geometry could influence the shear forces on the substrate's surface during alginate impact and, in consequence, improve the vitality of immobilized cells. Completed by a video microscope and software language, tailored patterns of immobilized cells can be produced.

The alginate dispenser could also assist cryopreservation protocols for adherent mammalian cells. After freeze/thaw cycles, cells tend to round off and consequently get lost in suspension. Thin alginate layers could hold cells onto the substrate. The first freeze/thaw cycles show, after 4 weeks of preservation at -80°C, reliability of alginate spots after thawing. The dispenser and integrated industrial microscope should allow structuring of nonplanar surfaces, which is beyond current commercial techniques (i.e., µContact printing; Reference 21). Cells do not survive passage through the valve, probably due to the shear forces. Recent literature shows the difficulties of handling high-end hardware and biological cells at the same time (22).

We have developed a versatile novel technique that allows the dispensing of highly viscous alginates and other biologically active solutions onto substrates. With our currently optimized encapsulation process, we can dispense alginate onto adherent cells of different types under sterile conditions. Several tests of selected properties (proliferation, gene expression, metabolic activity, and mechanical contraction) prove the functionality of cells after the encapsulation procedure. Structuring of substrates and dispensing of ECM-derived gels is also possible.

ACKNOWLEDGMENTS

This work was supported by a grant from the Federal Ministry of Education and Research (BMBF) given to H.Z. (grant no. 03N8707). The authors thank Alisa Katsen-Globa, Department for Cryobiophysics and Cryotechnology, Fraunhofer Institute for Biomedical Engineering, for her support in performing immunohistochemistry. The authors gratefully acknowledge Hagen Thielecke and Heiko Büth, Department for Biohybrid Systems, Fraunhofer Institute for Biomedical Engineering, for their scientific support concerning chicken cardiomyocytes.

COMPETING INTERESTS STATEMENT

S.F. is a CEO of GeSiM mbH, manufacturer of the Nano-Plotter dispensing system.

REFERENCES

1. **Zimmermann, H., D. Zimmermann, R. Reuss, P.J. Feilen, B. Manz, A. Katsen, M. Weber, F.R. Ihmig, et al.** 2005. Towards a medically approved technology for alginate-based microcapsules allowing long-term immunoisolated transplantation. J. Mater. Sci. Mater. Med. *16*:491-501.
2. **Zhang, H., E. Tumarkin, R. Peerani, Z. Nie, R.M.A. Sullan, G.C. Walker, and E. Kumacheva.** 2006. Microfluidic production of biopolymer microcapsules with controlled morphology. J. Am. Chem. Soc. *128*:12205-12210.
3. **Zhou, Y., T. Sun, M. Chan, J. Zhang, Z. Han, X. Wang, Y. Toh, J.P. Chen, and H. Yu.** 2005. Scalable encapsulation of hepatocytes by electrostatic spraying. J. Biotechnol. *117*:99-109.
4. **Orive, G., A.R. Gascón, R.M. Hernández, M. Igartua, and J.L. Pedraz.** 2003. Cell microencapsulation technology for biomedi-

cal purposes: novel insights and challenges. Trends Pharmacol. Sci. *24*:207-210.
5. **Pandey, R., Z. Ahmad, S. Sharma, and G.K. Khuller.** 2005. Nano-encapsulation of azole antifungals: potential applications to improve oral drug delivery. Int. J. Pharm. *301*:268-276.
6. **Gibbs, B.F., S. Kermasha, I. Alli, and C.N. Mulligan.** 1999. Encapsulation in the food industry: a review. Int. J. Food Sci. Nutr. *50*:213-224.
7. **Nuttelman, C.R., M.C. Tripodi, and K.S. Anseth.** 2005. Synthetic hydrogel niches that promote hMSC viability. Matrix Biol. *24*:208-218.
8. **Shirai, Y., K. Hashimoto, H. Kawahara, R. Sasaki, K. Hitomi, and H. Chiba.** 1989. Production of erythropoietin by BHK cells growing on the microcarriers trapped in alginate gel beads. Cytotechnology *2*:141-145.
9. **Gerecht-Nir, S., S. Cohen, A. Ziskind, and J. Itskovitz-Eldor.** 2004. Three-dimensional porous alginate scaffolds provide a conducive environment for generation of well-vascularized embryoid bodies from human embryonic stem cells. Biotechnol. Bioeng. *88*:313-320.
10. **Reddig, P.J. and R.L. Juliano.** 2005. Clinging to life: cell to matrix adhesion and cell survival. Cancer Metastasis Rev. *24*:425-439.
11. **Lutolf, M.P. and J.A. Hubbell.** 2005. Synthetic biomaterials as instructive extracellular microenvironments for morphogenesis in tissue engineering. Nat. Biotechnol. *23*:47-55.
12. **Thomas, F.T., J.L. Contreras, G. Bilbao, C. Ricordi, D. Curiel, and J.M. Thomas.** 1999. Anoikis, extracellular matrix, and apoptosis factors in isolated cell transplantation. Surgery *126*:299-304.
13. **Douma, S., T. Van Laar, J. Zevenhoven, R. Meuwissen, E.Van Garderen, and D.S. Peeper.** 2004. Suppression of anoikis and induction of metastasis by the neurotrophic receptor trkb. Nature *430*:1034-1039.
14. **Otsuka, H. and M. Moskowitz.** 1975. Arrest of 3t3 cells in g1 phase in suspension culture. J. Cell. Physiol. *87*:213-219.
15. **Re, F., A. Zanetti, M. Sironi, N. Polentarutti, L. Lanfrancone, E. Dejana, and F. Colotta.** 1994. Inhibition of anchorage-dependent cell spreading triggers apoptosis in cultured human endothelial cells. J. Cell Biol. *127*:537-546.
16. **Abramoff, M.D., P.J. Magelhaes, and S.J. Ram.** 2004. Image processing with imagej. Biophotonics International *11*:36-42.
17. **García, A.J. and C.D. Reyes.** 2005. Bioadhesive surfaces to promote osteoblast differentiation and bone formation. J. Dent. Res. *84*:407-413.
18. **Fischer, D., Y. Li, B. Ahlemeyer, J. Krieglstein, and T. Kissel.** 2003. In vitro cytotoxicity testing of polycations: influence of polymer structure on cell viability and hemolysis. Biomaterials *24*:1121-1131.
19. **Range, K. and F. Feuillebois.** 1998. Influence of surface roughness on liquid drop impact. J. Colloid Interface Sci. *203*:16-30.
20. **Torri, D., M. Sfalanga, and M. Del Sette.** 1987. Splash detachment: runoff depth and soil cohesion. Catena *14*:149-155.
21. **Truskett, V.N. and M.P.C. Watts.** 2006. Trends in imprint lithography for biological applications. Trends Biotechnol. *24*:312-317.
22. **Calvert, P.** 2007. Printing cells. Science *318*:208-209.

Received 5 November 2007; accepted 10 October 2008.

Address correspondence to Heiko Zimmermann, Department for Cryobiophysics and Cryotechnology, Fraunhofer Institute for Biomedical Engineering, Ensheimer Str. 48, 66386 St. Ingbert, Germany. e-mail: heiko.zimmermann@ibmt.fraunhofer.de